PROTEINS: Structure, Function, and Genetics 10:33–49 (1991)

The Crystal Structure of the "Open" and the "Closed" Conformation of the Flexible Loop of Trypanosomal Triosephosphate Isomerase

Rik K. Wierenga,[1] Martin E.M. Noble,[1] Johan P.M. Postma,[1] Hillie Groendijk,[2] Kor H. Kalk,[2] Wim G.J. Hol,[2] and Fred R. Opperdoes[3]

[1]European Molecular Biology Laboratory, Meyerhofstrasse 1, D-6900 Heidelberg, Federal Republic of Germany, [2]Laboratory of Chemical Physics, University of Groningen, Nijenborgh 16, NL-9747 AG Groningen, The Netherlands, and [3]ICP-TROP/7439, Avenue Hippocrate 74, B-1200 Brussels, Belgium

ABSTRACT **Triosephosphate isomerase has an important loop near the active site which can exist in a "closed" and in an "open" conformation. Here we describe the structural properties of this "flexible" loop observed in two different structures of trypanosomal triosephosphate isomerase. Trypanosomal triosephosphate isomerase, crystallized in the presence of 2.4 *M* ammonium sulfate, packs as an asymmetric dimer of 54,000 Da in the crystallographic asymmetric unit. Due to different crystal contacts, peptide 167–180 (the flexible loop of subunit-1) is an open conformation, whereas in subunit-2, this peptide (residues 467–480) is in a closed conformation. In the closed conformation, a hydrogen bond exists between the tip of the loop and a well-defined sulfate ion which is bound to the active site of subunit-2. Such an active site sulfate is not present in subunit-1 due to crystal contacts. When the native (2.4 M ammonium sulfate) crystals are transferred to a sulfate-free mother liquor, the flexible loop of subunit-2 adopts the open conformation. From a closed starting model, this open conformation was discovered through molecular dynamics refinement without manual intervention, despite involving Cα shifts of up to 7 Å. The tip of the loop, residues 472, 473, 474, and 475, moves as a rigid body. Our analysis shows that in this crystal form the flexible loop of subunit-2 faces a solvent channel. Therefore the open and the closed conformations of this flexible loop are virtually unaffected by crystal contacts. The actual observed conformation depends only on the absence or presence of a suitable ligand in the active site.**

Key words: TIM, molecular dynamics refinement, loop movement, conformational change, crystal contacts, sleeping sickness, suramine

INTRODUCTION

Triosephosphate isomerase (TIM) is an important glycolytic enzyme, consisting of two identical subunits. The crystal structures of chicken TIM,[1] yeast TIM,[2] and trypanosomal TIM[3] have been determined to varying levels of precision. In each crystal form, the asymmetric unit consists of a complete dimer. Each subunit has a globular shape with two protruding loops. The globular part is formed by 8 βα units, which fold up in a regular way such that the β-strands form an eight-stranded parallel β-barrel, surrounded on the outside by the 8 α-helices. The β-strands are numbered β1 to β8 and the α-helices α1 to α8 (Fig. 1). The two protruding loops are between β3 and α3 (the "interface" loop), and between β6 and α6 (the "flexible" loop). The interface loop is important for dimerization, since it fits into a complementary pocket of the other subunit of the dimer. It does not protrude into solution in the intact dimer.

The catalytic properties of TIM have been studied in great detail. Knowles and collaborators have shown that in vivo the rate-limiting steps are the on/off rates of the substrates and products.[4] Important catalytic functions have been ascribed to three different residues (for a review see reference 2): in chicken TIM these residues are Lys-13 (at the end of β1), His-95 (at the end of β4) and Glu-165 (at the end of β6). In trypanosomal TIM these residues are Lys-13, His-95, and Glu-167. The sequence alignment of chicken TIM, yeast TIM, and trypanosomal TIM is given in Figure 2. In this paper we will refer to the trypanosomal sequence numbers. The catalytic residue Glu-167 is at the beginning of the flexible loop. Crystallographic studies have shown that this flexible loop folds over the active site in the presence of

Received March 12, 1990; revision accepted September 6, 1990.

Address reprint requests to Rik K. Wierenga, European Molecular Biology Laboratory, Meyerhofstrasse 1, D-6900 Heidelberg, Federal Republic of Germany.

Abbreviations used: TIM, triosephosphate isomerase (EC 5.3.1.1); DTT, dithiothreitol; EDTA, ethylenediaminetetracetic acid; MOPS, 3-(*N*-morpholino)-propane sulfonic acid; DHAP, dihydroxyacetone phosphate; PEG, polyethyleneglycol; rms, root mean square.

© 1991 WILEY-LISS, INC.

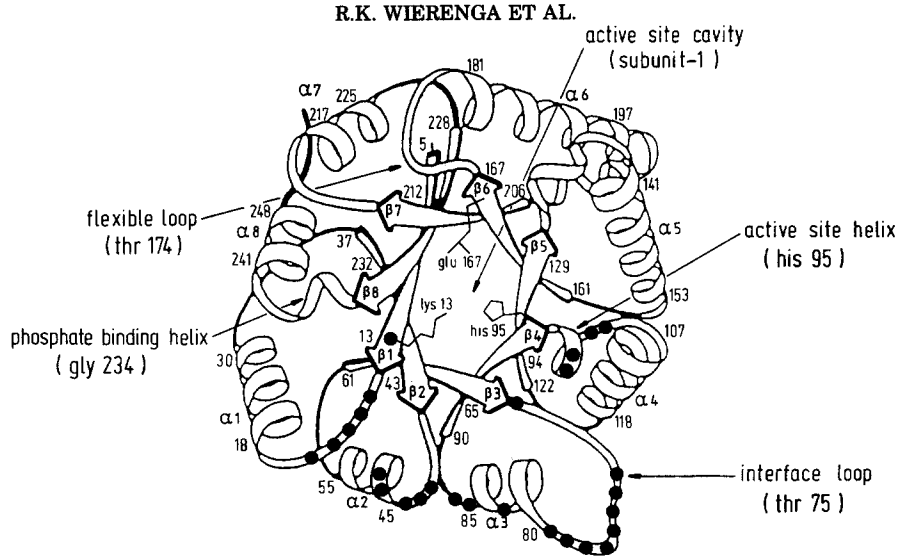

Fig. 1. A schematic drawing of subunit-1 of the TIM-dimer. The β-strands and α-helices of the 8 (βα) units are labeled as β1 to β8 and α1 to α8. The black dots indicate the positions of the dimer interface residues.[3] The interface loop fits in a cavity near the active site of the other subunit. The flexible loop can exist in an open and in a closed conformation. The approximate positions of the active site residues Lys-13, His-95, and Glu-167 are explicitly drawn. His-95 is at the beginning of the active site helix. The sulfate ion (Sul-555, see text) binds at the binding pocket for the phosphate moiety of the substrate analogues, which is at the N-terminus of the phosphate binding helix.

ligands.[2] Molecular dynamics calculations[5] suggest that the interactions between the ligand and the flexible loop atoms are sufficient to close this loop.

Chicken TIM has been crystallized in the presence of 2.4 M ammonium sulfate. The asymmetric unit contains one dimer, and both active sites contain a bound sulfate ion. In this crystal form, the flexible loops in both subunits are in an open conformation. When high concentrations of the substrate, dihydroxyacetone phosphate (DHAP), are added to the mother liquor, the crystals crack, but low resolution X-ray studies at 6 Å have shown that binding of DHAP in the active site of chicken TIM causes the loop to fold over the active site (in one of the two subunits), adopting the closed conformation.[2] The tip of the loop moves approximately 10 Å, to make a hydrogen bond with the phosphate moiety of DHAP. The crystals crack because the crystal contacts are disrupted when the loop conformation changes.[2]

Yeast TIM has been crystallized from a PEG 4000 solution containing approximately 0.5 M ammonium sulfate.[6] Before data collection these crystals are transferred to a sulfate-free mother liquor, with no effect on the diffraction pattern.[2] These crystals are well ordered, and a 1.9 Å refined structure has been determined by Petsko et al.[30] The flexible loop is in an open conformation in both subunits. Yeast TIM has also been cocrystallized with the substrate analogues phosphoglycolohydroxamate and 2-phosphoglycolate. The structures of these complexes have been refined at 1.9 (Petsko and co-workers, manuscript in preparation), and 2.5 Å,[31] respectively. In both complexes the flexible loop is in a closed conformation in each subunit, with both active sites occupied by ligand.

Here we describe the results of crystallographic studies with trypanosomal TIM. Trypanosomes are unicellular eukaryotic organisms.[7] They are the causative agents of various tropical diseases, including sleeping sickness in man and nagana in cattle. Drugs such as suramine which are currently used in the treatment of trypanosome-induced diseases are not satisfactory.[7] It has been established that the enzymes of the glycolytic pathway in this organism have several unique properties, for example, these enzymes are sequestered in a microbody called the glycosome.[8] Compounds which inhibit the glycolytic pathway kill the trypanosome.[8] Therefore it is our hope that structural studies of trypanosomal glycolytic enzymes such as described here will contribute to the development of selective new drugs against these diseases.[9]

Trypanosomal TIM (abbreviated as "gTIM" because in the trypanosomes this enzyme occurs only in the glycosome) was purified as described by Misset et al.[10] Crystals of gTIM are grown in the presence of 2.4 M ammonium sulfate. We will refer to these crystals as the "native (2.4 M AS)" crystals. A method has been developed to transfer these crystals to a sulfate-free medium (the "sulfate-free" crys-

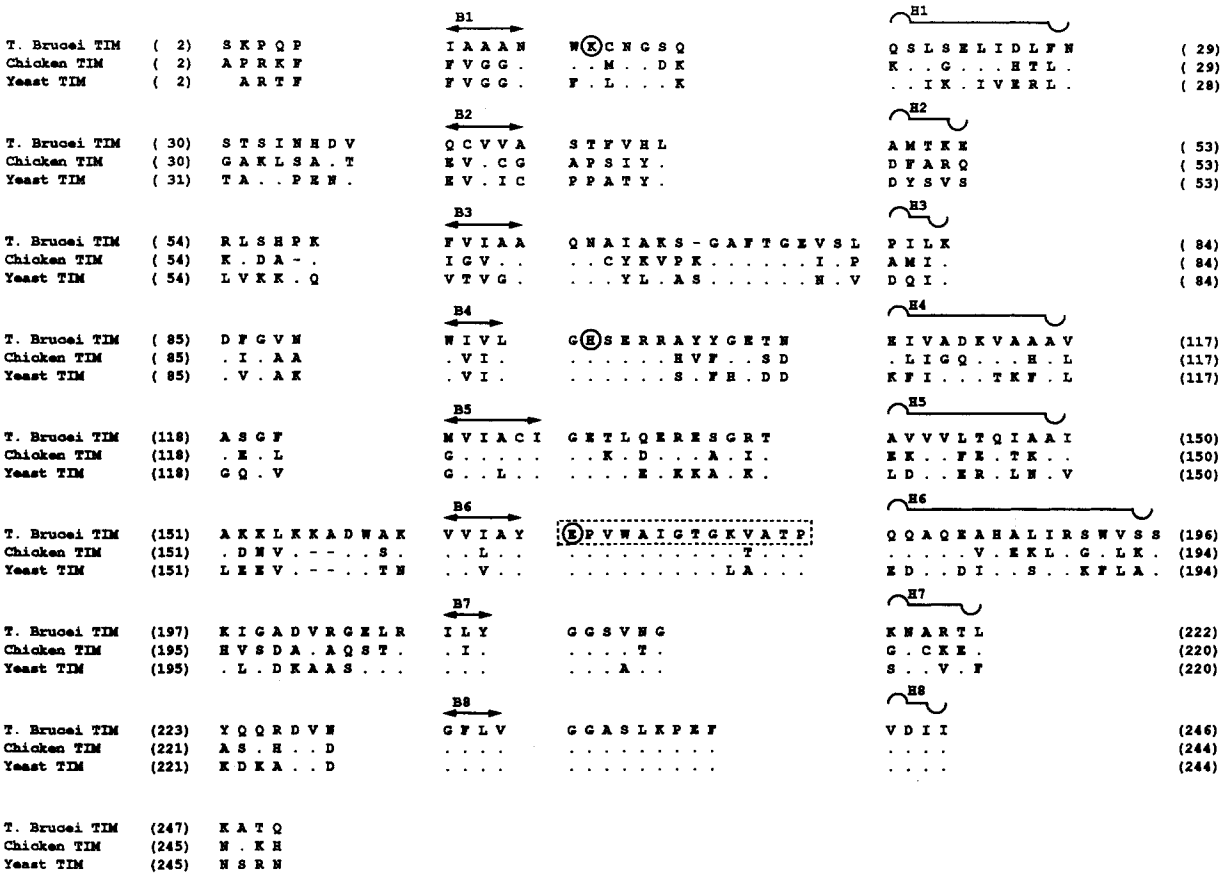

Fig. 2. The aligned sequences of trypanosomal TIM, chicken TIM, and yeast TIM. The β-strand and α-helix residues of the 8 βα-units used for superposition are specifically indicated. The secondary structure assignment is based on the structure of native (2.4 M AS) trypanosomal TIM according to the DSSP criteria of Kabsch and Sander.[29] The catalytic residues Lys-13, His-95, and Glu-167 are encircled. The 14 residues of the flexible loop are within a box of dashed lines.

tals). In this paper we will discuss the structural properties of the flexible loop as observed in the native (2.4 M AS) crystal and in the sulfate-free crystal.

MATERIALS AND METHODS

Determination of the Structure of the Native (2.4 M AS)-gTIM Structure

The native (2.4 M AS)-gTIM crystals grow at pH 7.0 and in a 0.2 M MOPS buffer, containing 1 mM EDTA, 1 mM sodium azide, 1 mM DTT, and 2.4 M ammonium sulfate.[11] The structure determination at 2.4 Å has been described previously.[3] The refinement of this structure at high resolution is now nearly complete. The refinement procedure, which will be published elsewhere, has been carried out with a 1.83 Å dataset (90% complete to 1.9 Å) collected by oscillation photography using the Daresbury synchrotron X-ray source. The *R*-merge of the complete dataset is 8.9% (Table I). The final stages of the refinement of positional and individual atomic thermal parameters, using the TNT refinement package,[12] were followed by careful examination of SIGMAA weighted $2F_o$-F_c electron density maps[13] on an Evans and Sutherland PS390 using FRODO.[14] Numerous rounds of restrained positional refinement and *B*-factor refinement, followed by interactive graphics sessions were carried out, until the $2F_o$-F_c, and F_o-F_c difference maps did not suggest further improvements. In this model, there are 4,088 atoms, consisting of one active site sulfate ion, 292 water molecules, one oxidized DTT molecule, one sulfate ion not near any active site, and 3,778 protein atoms. This model has an *R*-factor of 18.8% for all available data between 6 and 1.83 Å. Further refinement statistics are shown in Table I. All amino acid residues could be built into the electron density map, including residues with high *B*-factors, as shown in Figure 3. Details of the structural features of this structure will be published elsewhere.

Throughout this paper the following residue numbering scheme is used. Residues of subunit-1 are numbered from 2 to 250, whereas residues of subunit-2 have numbers from 302 to 550. The active site sulfate ion is labeled as Sul-555 (or S555). As will be

TABLE I. Crystallographic Data

		Native (2.4 M AS)	Sulfate-free
Unit cell	a(Å)	113.14	113.14
	b(Å)	97.69	96.48
	c(Å)	46.56	46.43
Data sets	Max resolution (Å)	1.83	2.8
	Number of measured data	122216	26975
	Number of unique data	38819	10369
	Completeness	90% (to 1.9 Å)	80% (to 2.8 Å)
	R-merge*	8.9%	6.5%
Refinement	$R^{\dagger}$	18.8% (6.0–1.83 Å)	13.9 (6.0–2.8 Å)
	Geometry-rms‡ (Å)	0.019	0.018
	rms delta B§ (Å^2)	7.0	7.4
	Number of atoms	4088	3808
	Protein atoms	3778	3778
	Solvent atoms	310	30

$$*R = \frac{\sum_h \sum_i |I_{hi} - \bar{I}_h|}{\sum_h \sum_i |\bar{I}_h|} \times 100\%.$$

$$^{\dagger}R = \frac{\sum_h |F_o - F_c|}{\sum_h |F_o|} \times 100\%.$$

‡Geometry-rms = rms deviation from ideal geometry for the covalent bonds.
§rms delta B = rms difference between the individual B-factors of covalently bonded atoms.

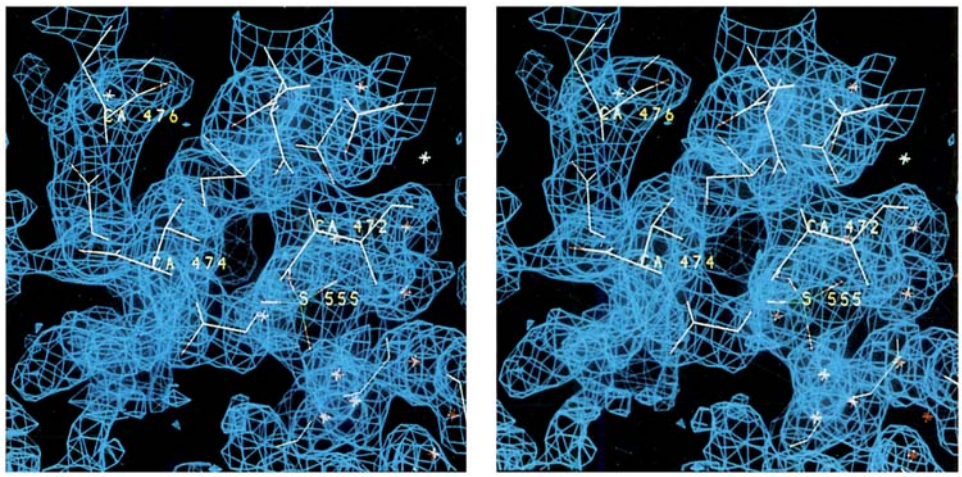

Fig. 3. The tip of the flexible loop of subunit-2 and the corresponding electron density map in the native (2.4 M AS) crystal. The map is a SIGMAA-weighted ($2F_o$-F_c) map[13] contoured at 1.5 times the rms value of the map density. All reflections between 25 and 1.83 Å have been included in the map calculation. The active site sulfate is labeled as S555.

discussed in later sections the two flexible loops in the two subunits have adopted two different conformations in this structure. This is schematically illustrated in Figure 4.

The Transfer of Native Crystals to a Sulfate-Free Mother Liquor, Data Collection, and Initial Refinement

The original purpose of this experiment was twofold:

1. To determine the mode of binding of 1-amino-naphthalene-4,6,8-trisulfonic acid. This is of interest since this negatively charged compound is an important building block of the antitrypanosomal drug suramine. It has been postulated that such a compound might interact specifically with the unique, positively charged patches on the surface of trypanosomal TIM.[15]

2. To establish the effect of the removal of the sulphate ion bound in the active site of subunit-2 in the native (2.4 M AS) structure.

The general protocol for the transfer of gTIM crys-

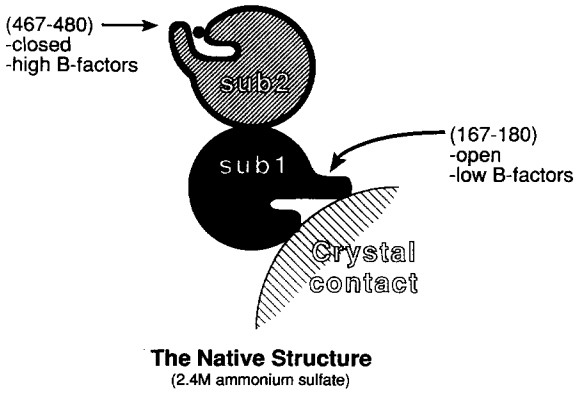

Fig. 4. Schematic drawing of the TIM dimer in the native (2.4 M AS) crystal. The flexible loops are labeled as (167–180) and (467–480). The major differences between subunit-1 and subunit-2 are indicated by the two different positions of the flexible loops. The black dot indicates the position of the well-defined sulfate ion (Sul-555) sitting at the entrance of the active site of subunit-2.

tals to another mother liquor has been described previously.[16] Following this protocol, the crystal to be used for data collection was transferred to a 44% PEG 6000 solution (44 g PEG 6000 in 100 g final mixture) in 0.2 M MOPS, pH 7.0, containing also 1 mM EDTA, 1 mM sodium azide, and 1 mM DTT, as well as 2 mM 1-aminonaphthalene-4,6,8-trisulfonic acid. After the transfer, the crystal was allowed to equilibrate in the new mother liquor for 2 weeks, during which period the mother liquor was replaced by a fresh solution at regular intervals. Subsequently the crystal was mounted and a 2.8 Å dataset was collected on the Groningen FAST area detector positioned on a GX21-rotating anode generator operating at 40 kV and 75 mA, using a graphite monochromator. Only one crystal was used for data collection. The detector was kept at 20.7°C to ensure good stability of the dark current. The crystal-to-detector distance was 70 mm, the detector was in a swing-out position with an angle of 17°. Frames of 0.15° were collected; the exposure time per frame was 3 min. First the crystal was rotated about a* over 96° and subsequently 36° of data were collected by rotating about b*. The frames were processed with MADNES,[17] and subsequently scaled and merged with programs of the Groningen BIOMOL package. The R-merge is 6.5% for all unique reflections between 25 and 2.8 Å (Table I).

Initially the structure was refined with the TNT refinement package, using an intermediate native structure as the starting model. First, the individual subunits of the starting model were refined as rigid bodies against data between 6 and 4 Å. This refinement produced an rms coordinate shift of 0.77 Å (Mean change in $x = -0.13$ Å, $y = -0.44$ Å, $z = -0.51$ Å), and resulted in a change in the R-factor from 35.9 to 29.2% for data between 6 and 4 Å. The rigid body constraint was then removed and 10 cycles of TNT positional refinement were carried out, yielding an R-factor of 22.2% for data between 6.0 and 2.8 Å. At this point, a $2F_o$-F_c map was calculated using the SIGMAA weighting scheme, and the fit of the model in density was examined on the PS390, using FRODO. It was observed that most regions of the protein fitted well into the density of this $2F_o$-F_c map, with the exception of the flexible loop of subunit-2, in particular residues 472–477, for which no reliable chain tracing was obvious.

MDX Refinement of the Sulfate-Free gTIM Structure

In order to determine the conformation of the flexible loop in the sulfate-free model, refinement was carried out using the technique of molecular dynamics refinement.[18] This technique allows sampling of a larger area of conformational space in the search for refinement minima than does conventional least squares refinement. The implementation of molecular dynamics refinement used here was the GROMOS MDX package.[19] The first stage in this refinement protocol is the relaxation of the starting structure to an energy minimum of the potential function used in the refinment. This was carried out in four steps of 50 cycles of energy minimization, with each step being accompanied by an increase in the maximum resolution of the included crystallographic data from 3.5 Å initially to 2.8 Å in the last step. To allow standardization, the course of the refinement has been monitored at all stages by calculation of the R-factor between 6.0 and 2.8 Å (Fig. 5). At the end of the energy minimization procedure, the R-factor calculated in this fashion was 23.8%. Further energy minimization of this structure was carried out at constant resolution and crystallographic weight to provide a reference point against which the results of molecular dynamics refinement could be assessed. The resulting structure (point A in Fig. 5) was used as the reference structure from which the extent of subunit-2 Cα movements were measured during the ensuing MDX protocol.

The parameters of MDX which alter the convergence characteristics of the refinement include the temperature of the run, the resolution range of included crystallographic data, and the weight assigned to the crystallographic pseudopotential. In the first part of our refinement scheme MDX was begun at low resolution and extended stepwise to the limit of the data available.[20] Throughout these calculations the atomic velocities were coupled to a thermal bath of constant temperature of 300 K, with a relaxation time of 0.1 psec.[21] Conformity with bond length constraints was ensured by application of the SHAKE algorithm.[22] At each resolution level, the weight applied to the crystallographic forces, governed by the parameter SIGF, was initially low [SIGF = 1.5× rms (F_o–F_c)], but was stepwise increased to a high value [SIGF = 0.75 × rms(F_o-F_c)].

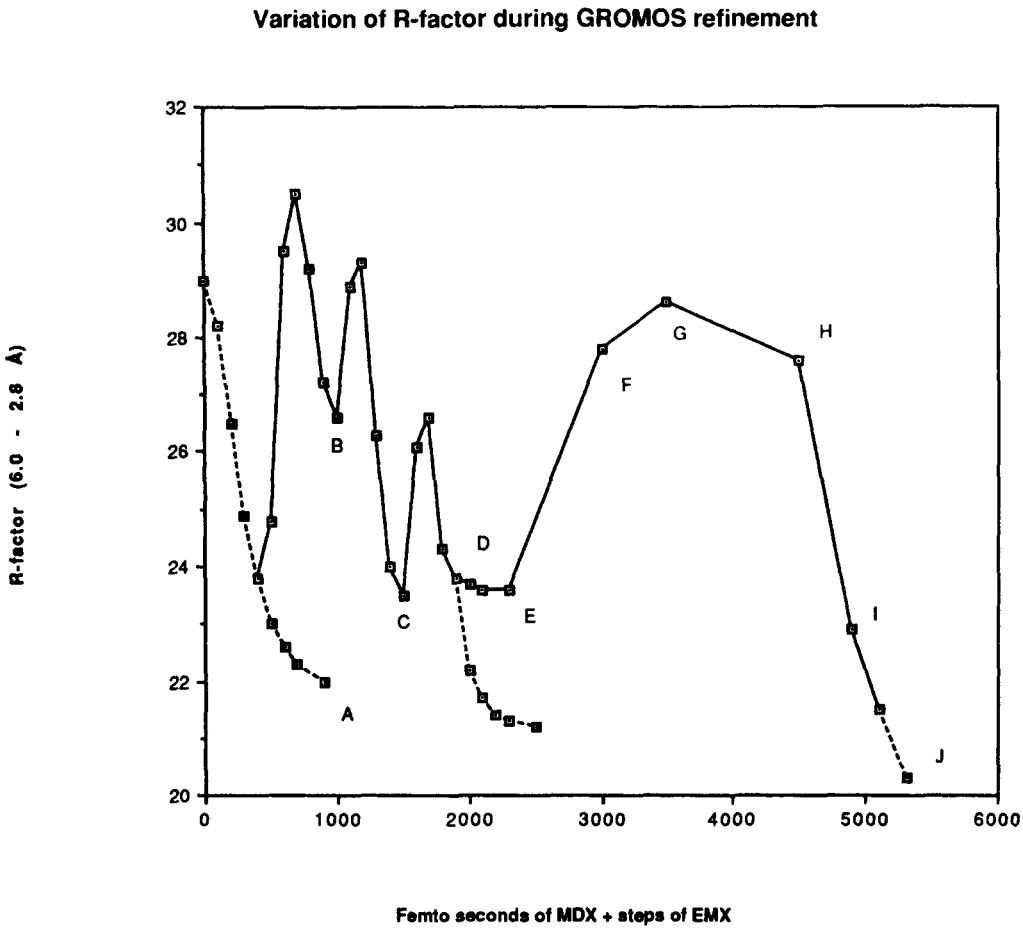

Fig. 5. The *R*-factor (vertical axis) for various intermediate structures is plotted as a function of the number of GROMOS steps. The EMX steps are indicated with dotted lines, the MDX steps (femtoseconds) are in solid lines. All *R*-factors are calculated for all the data between 6.0 and 2.8 Å. The details of the refinement are explained in the text.

The variation of the *R*-factor during this protocol is shown in Figure 5, with points B, C, and D representing the *R*-factors after the last cycles of MDX refinement at resolutions of 3.5, 3.1, and 2.8 Å, respectively. The evolution of the changes in backbone Cα positions along subunit-2 is shown in Figure 6, sampled at the same time points as for the analysis of *R*-factor during refinement.

From point D, energy minimization was carried out for 300 cycles to yield a structure of final *R*-factor 21.2%. This structure was used to phase the calculation of a new $2F_o$-F_c map. Examination of the new map and the new model revealed that although residues at the edges of the flexible loop had moved considerably (Fig. 6, line D), and were now in satisfactory density, the path of residues at the tip of the loop remained untraceable. It was, however, apparent that the residues now satisfactorily relocated had adopted a characteristic open conformation, most clearly seen for the side chain of Trp-170.

The untraceability of the flexible loop tip residues suggested that a further change in conformation might be required. Nevertheless continuation of the MDX-refinement did not result in further significant improvement of the structure (see point E in Fig. 5). Therefore a "simulated annealing" protocol was used.[23] The first stage in this protocol involved increasing the simulated temperature of the system. This was done by changing this temperature from 300 to 1000 K, with an unaltered temperature relaxation time of 0.1 psec. The temperature increase was implemented during an MDX run of approximately 1 psec. Annealing (points H,I) involves the slow reduction of the temperature of the system, achieved by decreasing the simulated temperature to 100 K, and increasing the temperature relaxation time to 0.4 psec.

The atomic *B*-factor set used up to point E in the refinement was derived from the starting native model. This set ascribed high thermal parameters to the flexible loop residues, thus making these residues comparatively insensitive to the crystallo-

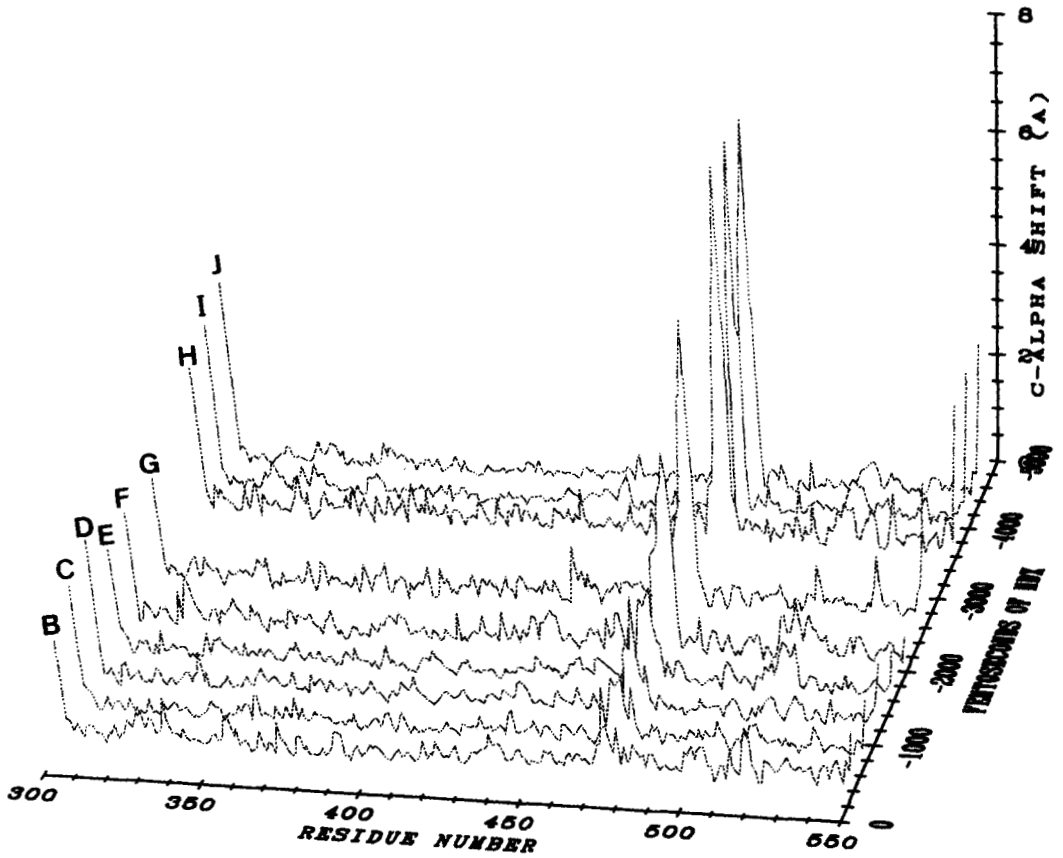

Fig. 6. Three-dimensional shiftplot of the subunit-2 Cα atoms at various stages of the GROMOS refinement of the sulfate-free structure. The Cα positional differences are plotted on the vertical axis with respect to the reference model (model A of Fig. 5). These differences are plotted for the various intermediate structures labeled as B to J (see also text), as a function of the residue numbers, which are plotted on the horizontal axis. The number of GROMOS steps from 0 to 5000 are plotted at the right side of the diagram.

graphic term in the energy function. In order to eleviate this effect, the *B*-factors were truncated at a maximum value of 50.0 Å^2. As an additional measure, a high crystallographic weight was chosen [SIGF = 0.75 × rms (F_o-F_c)], to ensure that correctly positioned atoms were held in position. The *R*-factor, and relative Cα shift were monitored throughout this protocol, yielding time points F to J (Figs. 5, 6). The outstanding feature of the Cα coordinate difference plot was seen to be the movement of residues at the tip of the flexible loop of subunit two, the movement being essentially complete by the end of the heating/equilibration stage (line H, Fig. 6). Energy minimization was carried out on the structure resulting from the annealing process, leading to a model with an *R*-factor of 20.3% between 6.0 and 2.8 Å (point J). A map calculated using this structure as a phasing model showed good, although broken, density for the flexible loop. The molecular dynamics protocol had allowed the correct repositioning of a loop of more than 10 residues, including a maximum Cα shift of approximately 7 Å, while retaining the generally correct conformation of the rest of the protein.

Further improvement of the structure was achieved by repeated cycles of TNT refinement alternating with interactive model building. In the course of manual rebuilding, three peptide bonds were rotated through approximately 180°, and the extreme N and C terminal residues of both subunits were rebuilt. In all cases the adjustment resulted in an improved fit in density, and increased the similarity of the model to the pre-MDX model. Thus these alterations reflected correction of errors introduced into the structure by the application of molecular dynamics. In addition, 30 water molecules were added to the model. These were selected on the basis of stereochemical feasibility from a list of the highest peaks in an F_o-F_c map.

None of these measures led to sufficient improvement in the phasing model to produce unbroken electron density in the region of the flexible loop of subunit two. This problem was finally overcome by inclusion of the low-resolution reflection data into the map calculation procedure. The correct phasing of the low resolution reflections, involved using the bulk solvent model of Fermi et al.[24] In this scheme, F_c values calculated from an enveloped continuum

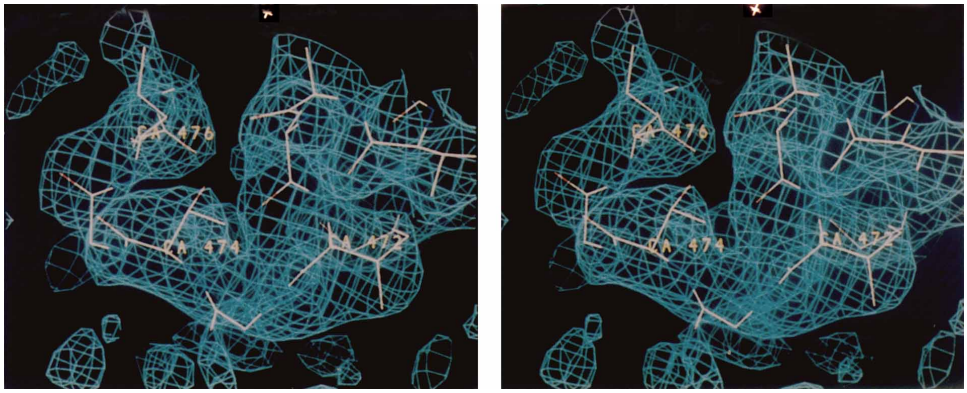

Fig. 7. The tip of the flexible loop of subunit-2 and the corresponding electron density map for the sulfate-free crystal. The map is a SIGMAA-weighted ($2F_o$-F_c) map, contoured at 1.5 times the rms value of the map density. All reflections between 25.0 and 2.8 Å have been included in the map calculation. To improve the phases of the low resolution data, a model for the solvent continuum has been used.[23]

of bulk solvent are vectorially scaled and added to the F_c set calculated from the protein atomic coordinates, in order to provide good phase information for the low resolution reflections. The map calculated in this fashion does have continuous density for the tip of the flexible loop, and therefore confirms the model for the flexible loop which had been derived from molecular dynamics and interactive model building.

TNT refinement of the structure between graphics sessions also included refinement of atomic thermal parameters. This involves the refinement of more than 15,000 parameters against less than 10,000 reflections between 6.0 and 2.8 Å. This is clearly an underdetermined problem. In such a low resolution structure, it is uncertain if individual atomic thermal factors can be refined to meaningful values. However, the thermal parameters were refined under imposed correlation between parameter values for covalently bonded atom pairs. Subsequent analysis of the results showed that refinement of thermal parameters of the 2.8 Å structure, starting from a state in which each atom had a temperature factor of 25 Å^2, leads to average B-factors per residue with a correlation coefficient of 0.8 when compared with the average B-factors per residue determined independently for the 1.8 Å resolution native (2.4 M AS) structure. A further analysis of the individual B factors shows that all of the high B-factor regions (Fig. 15) are in loops. We also observed that for external long side chains, the individual Bs for the end of the side chains are much higher than for the atoms close to the main chain. This is not true for buried long side chains. The ratio of the average B-factor for subunit-1 to the average B-factor of subunit-2 is 0.8 for both the sulfate-free and native 2.4 M AS structure. The lower average B-factor of subunit-1 can be related to the relatively larger proportion of subunit-1 involved in stabilizing crystal contacts. Clearly then the individual atomic B-factors are physically meaningful.

A total of 40 cycles of TNT positional refinement and 20 cycles of TNT B-factor refinement were carried out after the MDX stage, giving rise to a final R-factor of 13.9% for all data between 6.0 and 2.8 Å. All residues fit into their corresponding electron density, as shown in Figure 7 for residues at the tip of the flexible loop. A further assessment of the quality of the model is the degree to which it conforms to known stereochemical values. In this case, the covalent bond lengths of the model agreed with the expected values with an rms error of 0.018 Å, while the rms error in bond angles was 2.7°. At this point, the model contains 3,778 protein atoms and 30 water molecules. A comparison of these 30 waters in the sulfate-free structure with the equivalent positions in the native 2.4 M AS structure shows that 22 have direct equivalents within a cut off of 0.6 Å. Of the others, all but three form good hydrogen bonds with the protein and all are well defined in electron density.

For comparison, the R-factor of the final model assigned a single group B-factor, and with all waters deleted was calculated. Nor surprisingly this R-factor (22.3%) is significantly higher. A few cycles of positional refinement brought the R-factor back down to 20.1% with an rms change in atomic positions of only 0.08 Å.

Further evidence for the correctness of the eventual chain tracing achieved for the flexible loop in subunit-2 of the sulfate-free structure is presented in Figure 8. In this figure is shown the $2F_o$-F_c omit electron density map calculated with phases and F_c derived from model A (Fig. 5) leaving out residues 467–480: model A contains the coordinates available before initiation of molecular dynamics refinement. Superimposed on the electron density are the residues 471–477 of model A as well as of the final

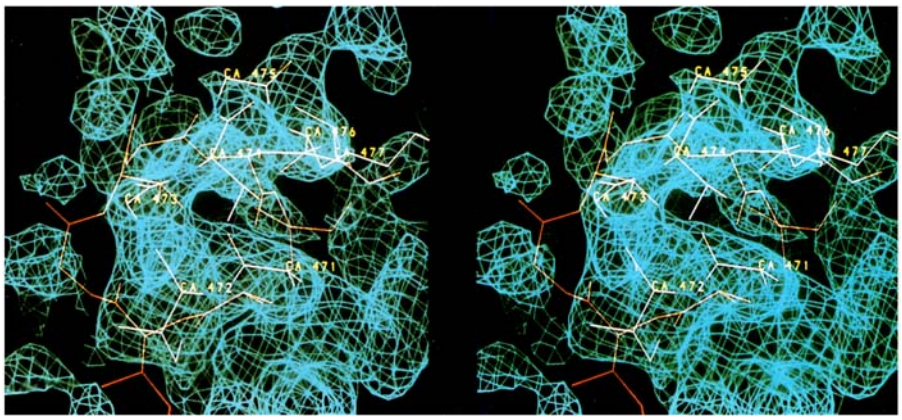

Fig. 8. The tip of the flexible loop of subunit-2 of model A (see Fig. 5), and of the final model (labeled) of the sulfate-free structure superimposed on an omit $2F_o$-F_c map calculated with the coordinates of model A (see Fig. 5) from which residues 467–480 have been deleted. All observed reflections between 25 and 2.8 Å have been included in the map synthesis. The map is contoured at a similar level to that used in Figure 7.

model. In this omit map, the tip of the flexible loop of the final model is clearly in positive density, which shows that the information for the final chain tracing was already present at this stage of the refinement.

The final difference map does not suggest in any way a potential mode of binding for 1-aminonaphthalene-4,6,8-trisulfonic acid. Also, $2F_o$-F_c and F_o-F_c maps suggest that the sulfate ion, found in the active site of subunit-2 of the native structure, is absent from this structure. Therefore, in the following discussions of the refined structure, we will concentrate on the new conformation of the flexible loop near the active site of subunit-2. It will be shown that in this sulfate-free crystal, the flexible loop is in an open conformation in both subunits.

RESULTS

The Structure of the Flexible Loop

After the refinement of the two different structures it is now possible to compare the four different subunits. Here we will discuss three different aspects of this comparison:

1. The absence/presence of sulfate in the four active sites.
2. The structural differences and similarities of the four flexible loops.
3. The differences in *B*-factors of the four flexible loops.

The absence/presence of sulfate in the four active sites

First we will discuss the native (2.4 M AS) structure. Only in the active site of subunit-2 is a well-defined sulfate ion present. This sulfate ion is stabilized by a hydrogen bond between a sulfate oxygen atom and the flexible loop. Due to different crystal contacts the situation in the active site of subunit-1 is different: at the equivalent position of the sulfate ion a water molecule has been refined. This well-defined water molecule interacts only weakly with neighboring atoms (the strongest interaction is with another water molecule at a distance of 3.5 Å). Therefore this water molecule could also be interpreted as a weakly bound sulfate ion. However, for two reasons this binding site is not a good sulfate-binding pocket. Firstly because of the nearby presence of the carboxylic acid moiety of a glutamic acid of a crystallographically related molecule; the distance between the water molecule and the carboxyl oxygen atom of this glutamic acid is 3.8 Å. Second, the packing of this crystallographically related molecule sterically precludes the closure of the flexible loop, which means that a sulfate ion in this binding pocket cannot be stabilized by a hydrogen bond with the flexible loop.

On transfer from 2.4 M ammonium sulphate to the sulfate-free mother liquor, the sulfate ion near the active site dissociates away. The electron density map of the sulfate-free crystal does not give any evidence for a sulfate ion at the equivalent position near the active sites of subunit-1 and subunit-2.

The structural differences and similarities of the four flexible loops

The 105 Cα atoms of the 8 βα units, as specified in Figure 2, superimpose very well. Pairwise comparisons of all subunits show rms differences for this set of Cα atoms of less than or equal to 0.3 Å. Using this superposition, rms positional difference plots for all residues were calculated in order to be able to quantify further the structural differences between the native (2.4 M AS) structure and the sulfate-free structure. No relevant differences were observed for

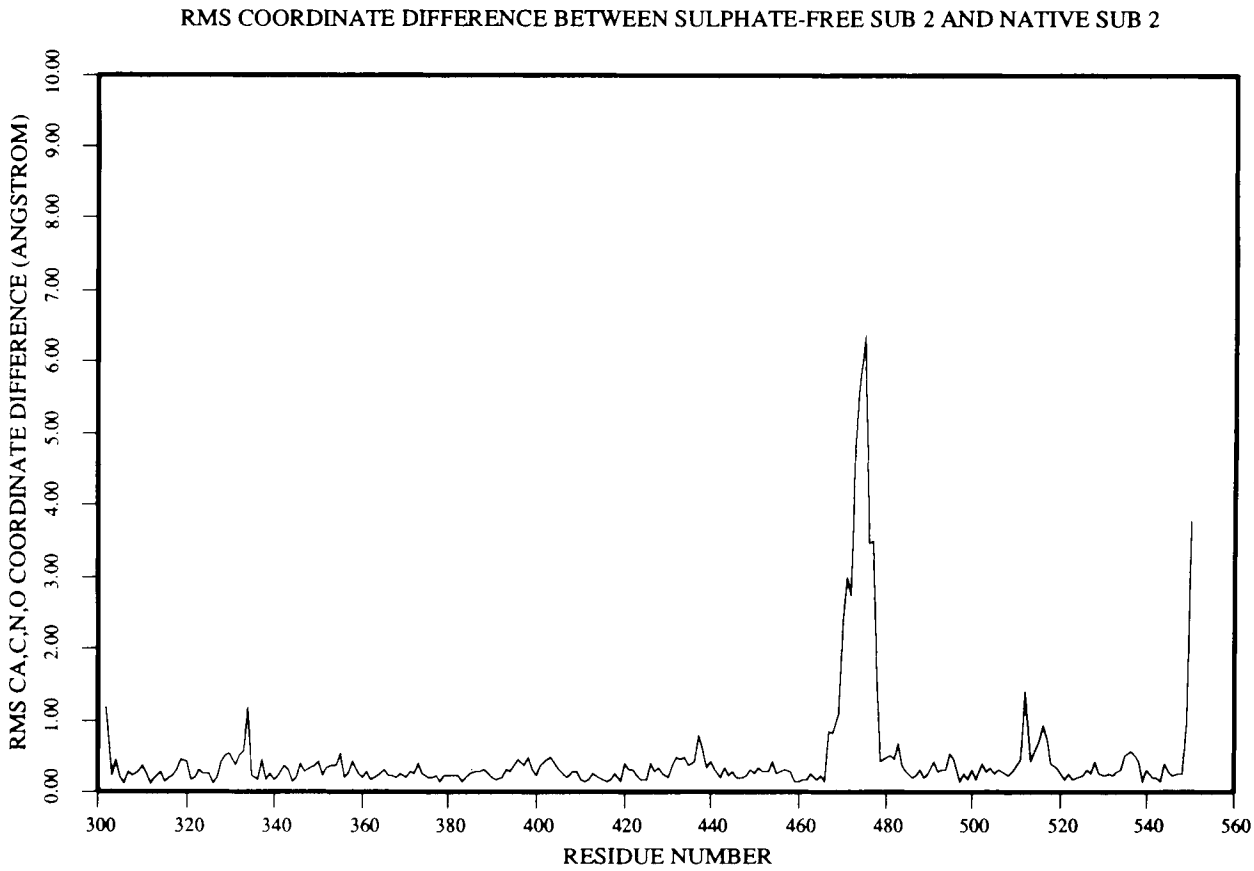

Fig. 9. The superimposed structure of subunit-2 (sulfate-free) is compared with subunit-2 (native; 2.4 M AS). The rms difference in position is plotted on the vertical axis (calculated for the N, Cα, C, O atoms per residue) as a function of residue number (horizontal axis).

the subunit-1 structures (data not shown), however the comparison of the subunit-2 structures (Fig. 9) shows clearly the major conformational change of the flexible loop region near residue 474 at the end of strand β6. Smaller structural differences can be observed in the region near residue 438 (at the end of strand β5), and near residue 512 (at the end of strand β7). These smaller structural differences are perhaps correlated with the larger movement of the flexible loop, whereas the small differences (Fig. 9) at the N-terminus, the C-terminus, and near residue 336 are far away from the active site.

Careful analysis of the superimposed structures indicates that the structural differences between the conformations of the flexible loop extend from residue 167 to residue 180. These residues adopt only two different conformations (in the four different subunits) as quantified in Table II. In this table rms positional differences are tabulated for the 56 main chain atoms of the 14 loop residues, after superposition on the basis of the 8 βα units. Apparently only residues 467–480 [subunit-2; native (2.4 M AS)] adopt a distinct closed conformation. In this conformation a good hydrogen bond (2.7 Å) is formed between O4(Sul-555) and N(Gly-473). The conformational differences between the open and the closed forms are depicted in Figure 10. Figure 11 shows that the open subunit-2 (sulfate-free) conformation is very similar to the open subunit-1 (native; 2.4 M AS) conformation. There are no peptide flips between the two conformations.

The schematic drawings of Figure 12 summarize the essential interactions of the closed and the open subunit-2 conformations. The subunit-2 flexible loops do not make any contacts with residues of subunit-1, also there are virtually no contacts with atoms from crystallographically related molecules. The only crystal contact interaction within 4 Å is a weak hydrogen bond (3.6 Å) of the NZ(Lys-476) in the sulfate-free structure. Also crystal contacts mediated via water molecules are absent. In the sulfate-free structure no water molecules have been found near the loop atoms. In the native (2.4 M AS) structure there are 9 water molecules near the loop atoms. Only one water (Wat-945; Fig. 12A) makes a good hydrogen bond with a loop atom; the other eight waters are weakly bound. None of these water molecules is involved in crystal contacts.

TABLE II. A Comparison of the Position of the 56 Main Chain Atoms of the Residues* of the Flexible Loop in the Four Different Subunits†: The rms Differences in Å Are Tabulated

	Native (2.4 M AS) (sub1)	Native (2.4 M AS) (sub 2)	Sulfate-free (sub1)	Sulfate-free (sub2)
Native (2.4 M AS)(sub1)	—	3.5	0.4	0.6
Native (2.4 M AS)(sub2)	3.5	—	3.5	3.3
Sulfate-free (sub1)	0.4	3.5	—	0.5
Sulfate-free (sub2)	0.6	3.3	0.5	—

*In subunit-1 residues 167–180; in subunit-2 residues 467–480.
†The superposition was done with rotational and translational parameters obtained from superimposing the 105 Cα atoms of the 8 (βα) units.

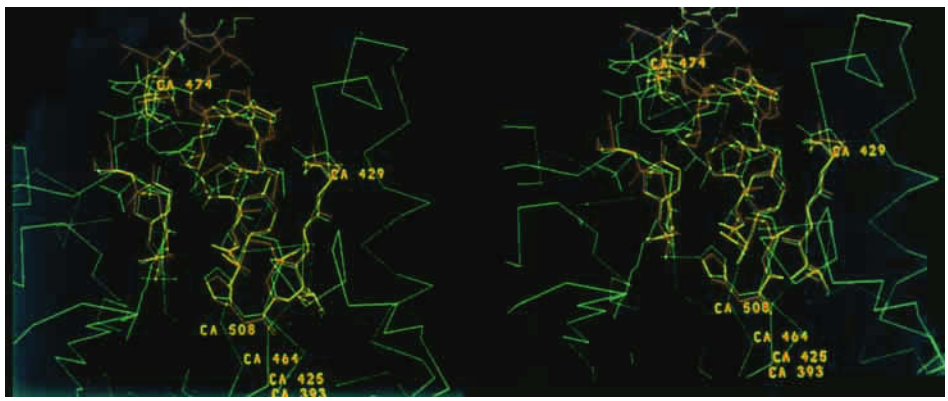

Fig. 10. Superposition of subunit-2 (sulfate-free), in red on top of subunit-2 (native; 2.4 M AS) in green. The labels 393, 425, 464, and 508 indicate approximately the C-terminal ends of the β-strands β4, β5, β6, and β7, respectively. Of both structures the main chain atoms plus side chain atoms of residues 395–396, 427–429, 466–479 (flexible loop), and 510–513 are shown explicitly. The positions of Lys-313 (green) and Sul-555 (green) are also shown. The orientation of the view is similar to Figure 1.

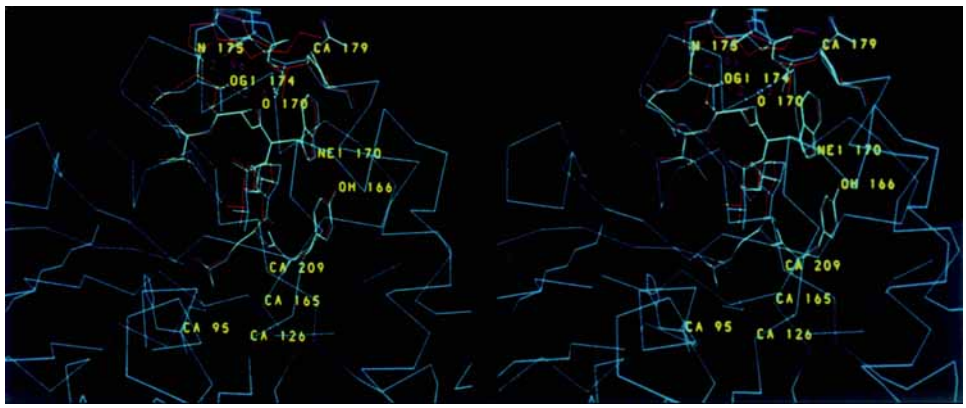

Fig. 11. Superposition of subunit-2 (sulfate-free), in red on top of subunit-1 (native) in blue. The labels 95, 126, 165, and 209 indicate approximately the C-terminal ends of the β-strands β4, β5, β6, and β7, respectively. The three active site residues Lys-13, His-95, and Glu-167 are shown in blue. All the atoms of both flexible loops are shown. The hydrogen bonds from OG1(Thr-174) to O(Trp-170), and from OG1(Thr-174) to N(Gly-175) are emphasized by the dotted lines. The atoms labeled NE1(170) and OH(166) also interact via a hydrogen bond. Note that the side chain atoms of the active site residue (Glu-167) do superimpose very well. The orientation of the view is similar to Figure 1.

In both conformations the main chain atoms are involved in only a few strong main chain–main chain hydrogen bonds. There exists a γ-turn between 467 and 469 (Fig. 12B) in the open structure, whereas in the closed conformation there exists a β-turn between residues 468 and 471. In the closed structure the main chain atoms are involved in more hydrogen bonds than in the open structure with atoms outside the loop region, such as those to O(Glu-429), OG(Ser-513), O4(Sul-555), and OH(Tyr-510)

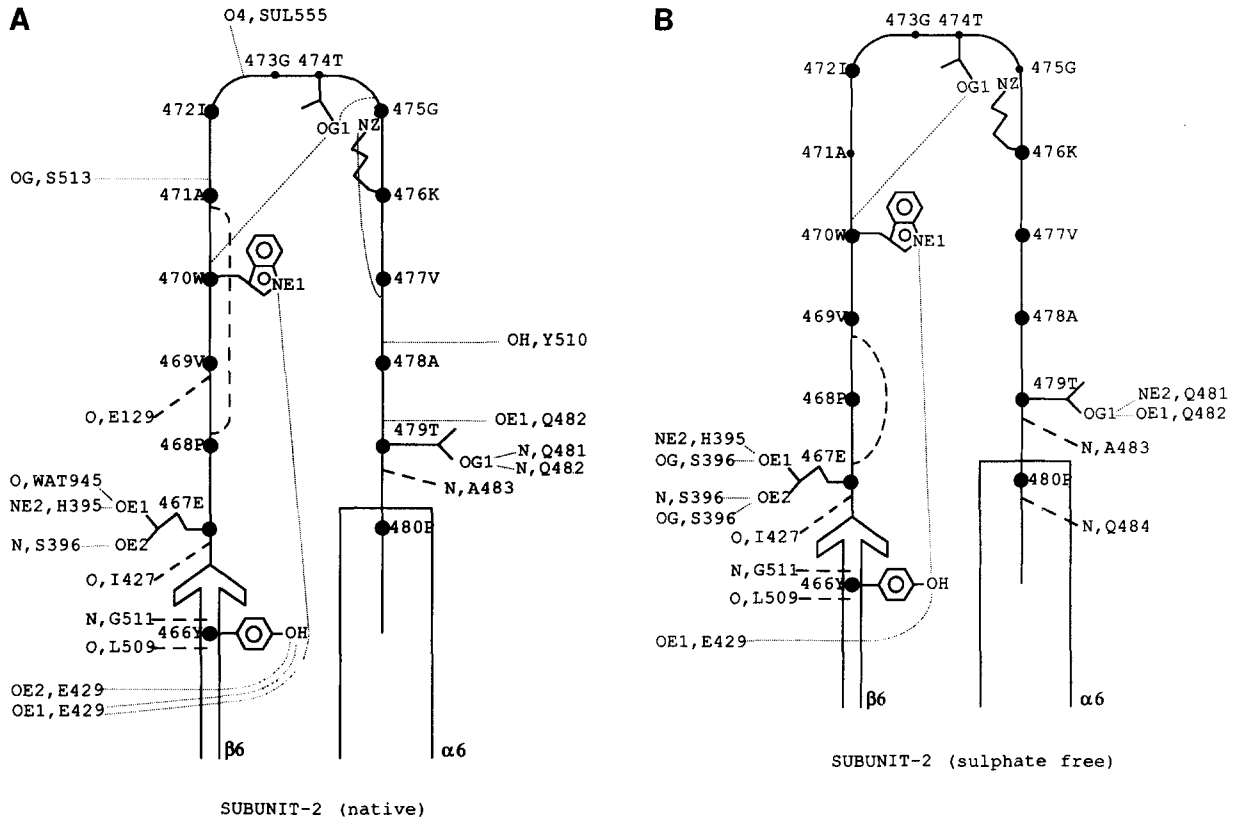

Fig. 12. Schematic drawing of the interactions of the flexible loop of subunit-2 (native; 2.4 M AS) **(A)** and subunit-2 (sulfate-free) **(B)**. The main chain–main chain hydrogen bonds have been calculated by the DSSP package.[28] Only hydrogen bonds with a calculated energy less than −1.9 kcal are visualized (dashed lines). Hydrogen bonds of side chain atoms (dotted lines) are visualized whenever the distances between hydrogen bond donor and hydrogen bond acceptor are less than 3.1 Å. Potential hydrogen bonds between the threonine OG1 atoms (474, 479) with main chain atoms of the same residue are not shown. Residues with a small dot at the Cα position have no contacts (within a 4 Å range) with any protein atoms outside the flexible loop region.

(Fig. 12). In both conformations all side chain atoms are hydrogen bonded to other protein atoms (Fig. 12), except for NZ of Lys-476, although the interactions do differ, for example for NE1(Trp-470). The two different conformations of Trp-470 are shown in Figure 10. It is interesting to see that despite the significant movement of Trp-470 and Thr-474, the hydrogen bond between OG1 (Thr-474) and O(Trp-470) remains intact. In the closed form, this distance is 3.0 Å whereas in the open form it is 2.6 Å.

A further analysis of the two different loop conformations has been carried out with the native (2.4 M AS) structure. This is shown in Figure 13, which shows the result of a fragment superposition carried out with the 16 main chain atoms of sequential stretches of four residues spanning the flexible loop. It can be seen that the structure of the tetrapeptide Ile-472–Gly-473–Thr-474–Gly-475 is the same in both conformations. The rms difference between the 16 main chain atoms of the superimposed tetrapeptide is only 0.2 Å, whereas the rms difference between all 56 main chain atoms of the superimposed loop (i.e., all 14 residues) is 1.2 Å. Apparently this fragment, which is at the tip of the loop, moves as a rigid body. This movement is caused by only small differences in the phi-psi angles of the residues just before and just after the tip of the loop, as shown in Figure 14. The largest differences are ψ(Lys-176) = +57 and ϕ(Val-177) = −38, which to some extent compensate each other.

The differences in B-factors of the four flexible loops

The open flexible loop conformations of subunit-2 and subunit-1 are very similar (Fig. 11), nevertheless, the *B*-factors are very different (data not shown). This observation can be correlated with the packing of the dimers in the crystals. The subunit-1 loops (low *B*-factors) are involved in crystal contacts. For example in both structures there exist direct and water-mediated hydrogen bonding interactions between Gly-175 and a crystallographically related molecule. The open subunit-2 loop and the closed subunit-2 loop are not stabilized by such interactions. The atoms at the tip of both subunit-2 loops have high *B*-factors, in particular the atoms of res-

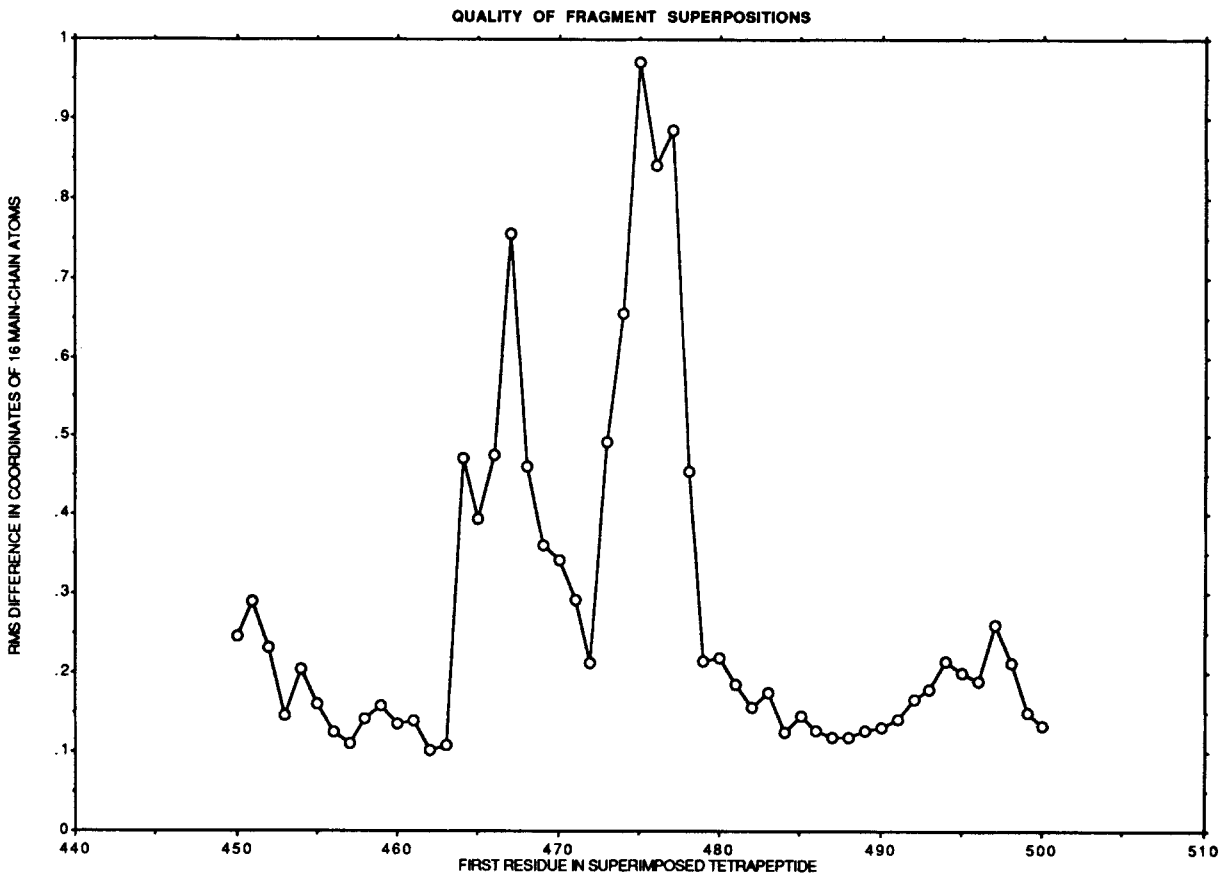

Fig. 13. Superposition of 4 residue fragments (main chain atoms only) of the native subunit-2 flexible loop on top of the native subunit-1 flexible loop. The rms differences (vertical axis) are plotted as a function of the residue number of the first residue of the fragment.

idues 170 to 178 (Fig. 15). The flanking regions of all flexible loops have a well-defined conformation.

Databank Analysis of the Structure of the Closed Flexible Loop

In the presence of substrate analogues, such as glycerol-3-phosphate, the flexible loop is also in a closed conformation, with a structure very similar to the structure of the native (2.4 M AS) subunit-2 loop but slightly shifted and with much lower individual *B*-factors.[32] In the closed state, the flexible loop contributes to the phosphate binding pocket, and the native (2.4 M AS) conformation can be considered to be the conformation of the loop when it is carrying out this function. In the databank of known structures there are many examples of phosphate binding loops, and a database search, using well-refined structures of the Brookhaven Protein Data Bank,[25] has been conducted to see if the closed flexible loop conformation is observed in any other structures. The search was done with all 16 main chain atoms of residues Ile-472–Gly-473–Thr-474–Gly-475. The results are tabulated in Table III; only the five conformations which fit best are listed. All the tabulated loops superimpose quite well (rms differences approximately 0.5 Å), and no peptide flips can be detected on visual inspection. The loops found in the database are not involved in phosphate binding, implying that this is not a conserved function of loops with this conformation. Interestingly, all these loops are stabilized by hydrogen bond interactions between a side chain and main chain atoms. For example, the hydrogen bond between OG1(Thr-474) and N(Gly-475) in trypanosomal TIM is replaced by an equivalent hydrogen bond between OD1(Asp-245) and N (Gly-246) in the structure of aspartic protease.[26]

A second database search was done with the main chain atoms of residues Pro-468–Val-469–Trp-470–Ala-471 of the native (2.4 M AS) structure. These residues form a type-III β-turn ($\phi 2 = -50$, $\psi 2 = -37$, $\phi 3 = -61$, $\psi 3 = -22$, compared with standard values of $\phi 2 = -60$, $\psi 2 = -30$, $\phi 3 = -60$, $\psi 3 = -30$[27]). This loop superimposes remarkably accurately upon similar β-turns in other structures. The rms difference for the 16 main chain atoms is less than 0.2 Å for the top five structures which fit best.

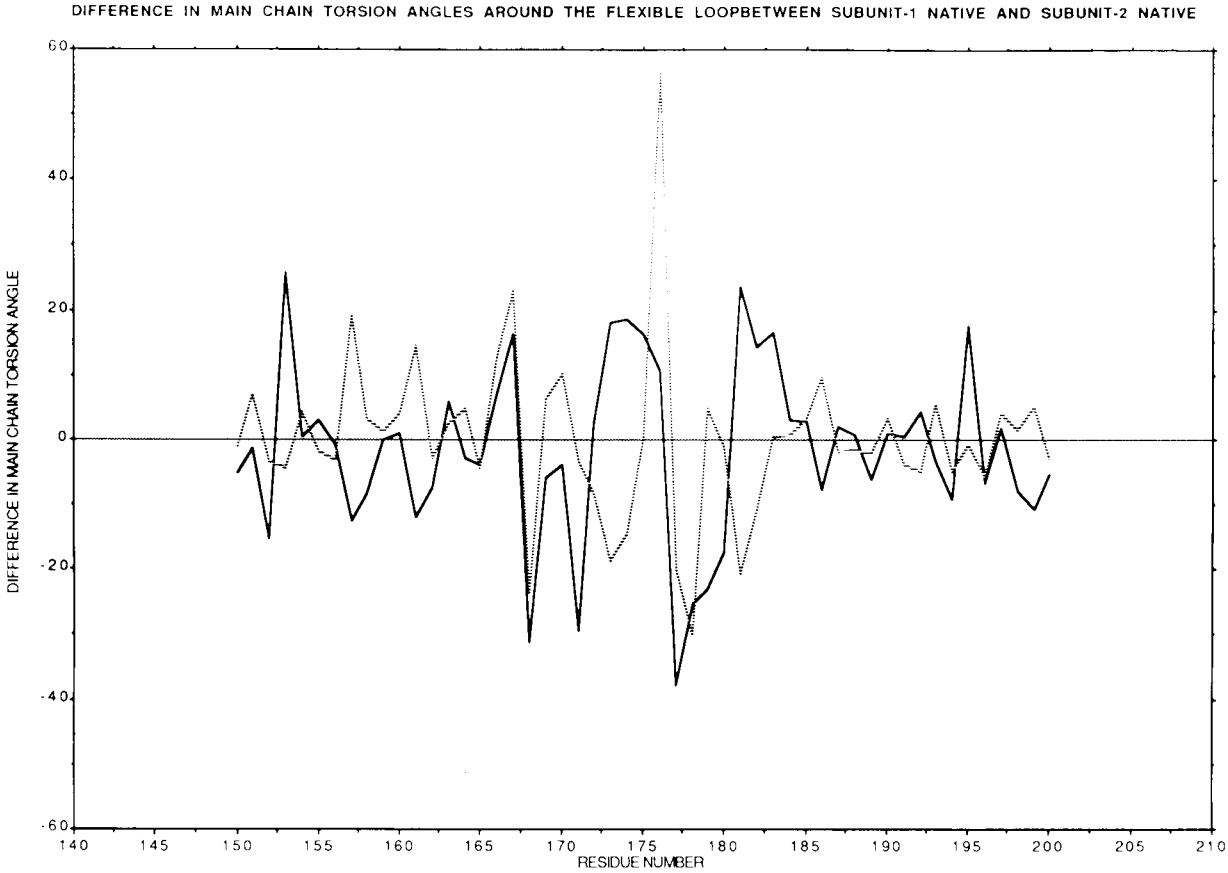

Fig. 14. Comparison of the ϕ and ψ values of the flexible loop residues of subunit-2 (native; 2.4 M AS) and subunit-1 (native; 2.4 M AS). The differences of ϕ (continuous line) and ψ (dotted line) are plotted on the vertical axis as a function of residue number.

DISCUSSION

Our analysis of the flexible loop shows that the subunit-2 loop faces a solvent channel in this crystal form and that its conformation is governed by the presence or absence of ligands. In the four different subunits of the two different crystal structures two different conformations of the flexible loop have been observed and the structural differences between these conformations have been described. In the sulfate-free structure as well as in subunit-1 (native; 2.4 M AS) the flexible loops are in an open conformation, but in the subunit-2 (native; 2.4 M AS)-structure the closed conformation is observed. The presence of a structurally asymmetrical dimer in the crystallographic asymmetric unit of the native (2.4 M AS) crystals is puzzling, because it can be assumed that in solution (2.4 M AS) both active sites are occupied by a sulfate ion (K_d = 4.5 mM) and that therefore, in solution, the flexible loop of both subunits is in a closed conformation. Clearly, in the absence of crystal contact interactions the loop favors the closed conformation in the presence of sulfate, as observed in subunit-2 (native; 2.4 M AS). The crystalline environment of the subunit-1 flexible loop destabilizes the closed conformation but stabilizes the open conformation. Evidently these crystal contact interactions are sufficiently strong to favor the open loop conformation.

Apparently, in trypanosomal TIM the hydrogen bond between the sulfate and Gly-473 triggers the conformational change of the flexible loop. The only reasonable alternative explanation would be that the presence of the sulfate ion changes the water structure in the active site which would subsequently effect the side chain conformation of the active site residue Glu-467 which would then induce the change in the loop conformation. In both states the flanking regions of the flexible loop (residues 467, 468, 469, 470, and 479, 480) have a well-defined, but different conformation.

In crystals of chicken TIM, the flexible loop is in an open conformation in the presence of sulfate; it closes only in the presence of phosphate or DHAP.[2] The structures of the open conformations of the flexible loop in chicken TIM and trypanosomal TIM are compared in Figure 16. For this comparison, the two subunits of chicken TIM (1TIM in the Protein Data Bank) have each been superimposed upon subunit-2 of trypanosomal TIM (sulfate free structure). For the superposition, the 105 Cα atoms of the eight ($\beta\alpha$)

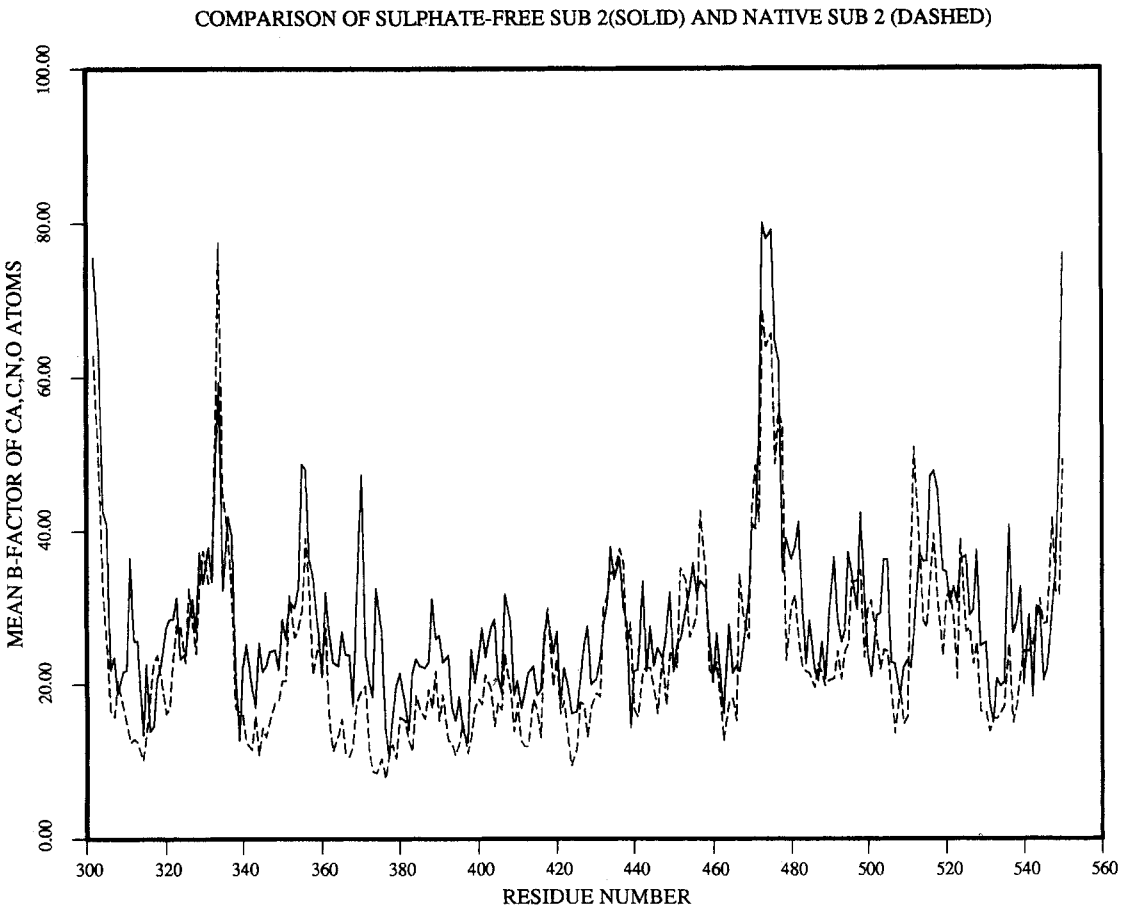

Fig. 15. Comparison of *B*-factors. The mean *B*-factor is plotted on the vertical axis (calculated for the N, Cα, C, O atoms) per residue as a function of residue number (horizontal axis). Solid line: subunit-2 (sulfate free). Dotted line: subunit-2 (native; 2.4 M AS).

TABLE III. Databank Search With Residues Ile-472–Gly-473–Thr-474–Gly-475 Using Well-Refined Structures From the Protein Data Bank[25]

Structure code	rms positional difference (Å)	Loop (residues; sequence)	Comments (resolution; *R*-factor; rms deviation from ideal geometry for the covalent bonds)
3APR	0.51	243–246 NGDG	Aspartic protease (1.8 Å; $R = 14.7\%$; rms = 0.009 Å)
2TMN	0.51	94–97 DGNN	Thermolysin (1.6 Å; $R = 17.9\%$; rms = 0.023 Å)
1SGC	0.53	73–76 LYNG	SGPA-protease (1.8 Å; $R = 12.3\%$)
6CHA	0.53	176–179 GASG	Chymotrypsin (1.8 Å; $R = 20\%$; rms = 0.030 Å)
1CCR	0.57	31–34 KGAG	Cytochrome *c* (1.5 Å; $R = 19\%$; rms = 0.020 Å)

units were used; these atoms superimpose with an rms error of 0.8 Å for both subunits. After superposition, the rms positional difference for the 56 main chain atoms of the flexible loops of chicken and trypanosomal TIMs are calculated to be 1.1 Å for subunit-1 and 1.4 Å for subunit-2. Apparently the open conformations of the flexible loop as observed in chicken TIM and in trypanosomal TIM are rather similar, despite the fact that at least one of the flexible loops of chicken TIM was difficult to build due to disorder.[2] It is intriguing that in the presence of sulfate the flexible loop is open in chicken TIM, but closed in subunit-2 of trypanosomal TIM. The crystallization conditions of chicken TIM (pH = 7.4, 2.4 M ammonium sulfate[1]) are very similar to the gTIM crystallization conditions, therefore only a detailed comparison of the crystal structures of chicken TIM and gTIM can establish if the difference in loop conformations in the presence of sulfate is due to differences in crystal packing or to intrinsic subtle differences between the two active sites. For example the chicken TIM-loop sequence is not identical to the

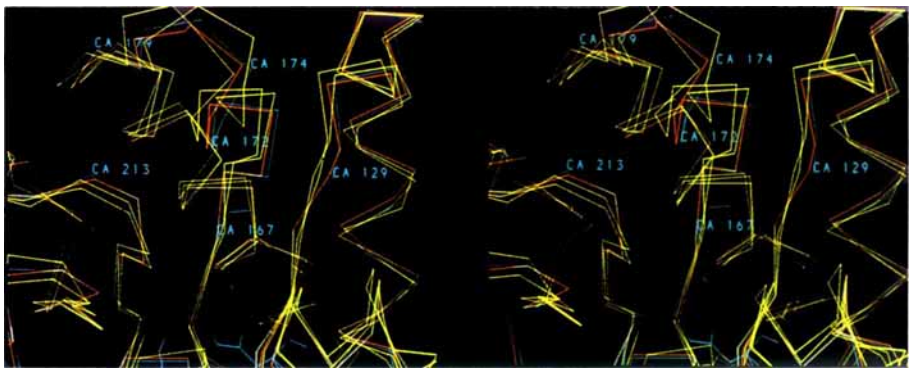

Fig. 16. Superposition of subunit-1 and subunit-2 of chicken TIM (in yellow) on subunit-2 (sulfate-free) in red. Subunit-1 of the native (2.4 M AS) structure is also shown (in blue). Some residues of the flexible loop of this subunit are labeled (labels 167 to 179); also the position of the catalytic residues of this subunit are explicitly indicated. Residue 129 is at the end of β-strand 5, the catalytic residue 167 is at the end of β-strand 6, and residue 213 is at the end of β-strand 7. The orientation of the molecule is similar to Figure 1.

gTIM-sequence, as Val-477 (Fig. 2) is replaced by a threonine in the chicken enzyme. Since human TIM is very similar to chicken TIM, such subtle differences could, in principle, be exploited in the development of selective drugs against trypanosomal diseases.

The crystallographic binding studies with the trisulfonated aminonaphthalene ring were also undertaken as a step towards the development of selective gTIM inhibitors. This compound selectively inhibits gTIM with a K_i of 0.3 mM. Nevertheless, no binding at the active site of subunit-2 or at any other potential binding site on the surface of gTIM is observed. As the active site of this subunit is quite accessible in the crystal, it has to be postulated that this compound binds at some distance from the active site, but that this potential binding site apparently cannot be occupied due to crystal contacts. Therefore only successful cocrystallization experiments can reveal the mode of binding of this compound.

The functional role of loop closure is not completely clear. It might have several functions. For example, it has been suggested that loop closure stabilizes the phosphate position, and, therefore, by mass action, prevents phosphate elimination,[28] which is an unwanted side reaction. Recent mutagenesis experiments[33] confirm that indeed, the absence of the loop enhances the undesired elimination reaction. Another function of the loop closure might be related to the position and flexibility of the active site residue Glu-467, which is at the beginning of the flexible loop. We observe that the conformation (Figs. 10, 11) and mobility (data not shown) of the side chain atoms of this residue are different in the closed and in the open form. In the open conformation the side chain atoms are well defined, but ill positioned for catalysis, whereas in the closed form the *B*-factors are much higher, indicating increased mobility. Further refinement of complexes of trypanosomal TIM with substrate analogues, such as glycerol-3-phosphate, might shed more light on the correlation between the conformation of the flexible loop and the structure and mobility of this crucial active site residue.

ACKNOWLEDGMENTS

It is a pleasure to acknowledge the help of Dr. Evans (solvent modeling), Drs. Lesk and Tramontano (databank search), and Dr. Vriend (processing of film data). Most important for this work has been the purification and characterization of trypanosomal TIM, which was done by Drs. Callens, Kuntz, and Lambeir at the ICP in Brussels. The compound 1-aminonaphthalenetrisulfonic acid was kindly given to use by Professor Nickel (Bonn). We thank Drs. Knowles, Lolis, and Petsko for stimulating discussions and sending us manuscripts prior to publication. The high resolution native TIM dataset was collected at the synchrotron facility in Daresbury (England) with the help of Randy Read, Steve Rule, and Myra Swarte. Processing of this dataset on the Cyber-205 computer at the SARA computer centre, Amsterdam was made possible by a special grant from the Dutch government. This research received financial support from the UNDP/World Bank/WHO Special Program for Research and Training in Tropical Diseases (to FRO and WGJH). The coordinates of the native (2.4 M AS) structure (2TIM) and the sulfate-free structure (3TIM) have been deposited in the Brookhaven Protein Data Bank.

REFERENCES

1. Banner, D.W., Bloomer, A.C., Petsko, G.A., Philips, D.C., Pogson, C.I., Wilson, I.A., Corran, P.H., Furth, A.J., Milman, J.D., Offord, R.E., Priddle, J.D., Waley, S.G. Structure of chicken muscle triosephosphate isomerase determined crystallographically at 2.5 Å resolution using the aminoacid sequence data. Nature (London) 255:609–614, 1975.
2. Alber, T., Banner, D.W., Bloomer, A.C., Petsko, G.A.,

Phillips, D.C., Rivers, P.S., Wilson, I.A. On the three-dimensional structure and catalytic mechanism of triosephosphate isomerase. Phil. Trans. R. Soc. London B293: 159–171, 1981.
3. Wierenga, R.K., Kalk, K.H., Hol., W.G.J. Structure determination of the glycosomal triosephosphate isomerase from *Trypanosoma brucei brucei* at 2.4Å resolution. J. Mol. Biol. 198:109–121, 1987.
4. Knowles, J.R., Albery, W.J. Perfection in enzyme catalysis: The energetics of triosephosphate isomerase. Acc. Chem. Res. 10:105–111, 1977.
5. Brown, F.K., Kollman, P.A. Molecular dynamics simulations of "loop-closing" in the enzyme triosephosphate isomerase. J. Mol. Biol. 198:533–546, 1987.
6. Alber, T., Hartman, F.C., Johnson, R.M., Petsko, G.A., Tsernoglou, D. Crystallization of yeast triosephosphate isomerase from polyethylene glycol. J. Biol. Chem. 256: 1356–1361, 1981.
7. Molyneux, D.H., Ashford, R.W. "The Biology of Trypanosoma and Leishmania, Parasites of Man and Domestic Animals." London: Taylor and Francis, 1983.
8. Opperdoes, F.R. Biochemical peculiarities of trypanosomes, African and South American. Br. Med. Bull. 41: 130–136, 1985.
9. Hol, W.G.J. Protein crystallography and computer graphics: Towards rational drug design. Angew. Chem. 25:767–778, 1986.
10. Misset, O., Bos, O.J.M., Opperdoes, F.R. Glycolytic enzymes of *Trypanosoma brucei*; simultaneous purification, intraglycosomal concentrations and physical properties. Eur. J. Biochem. 157:441–453, 1986.
11. Wierenga, R.K., Hol, W.G.J., Misset, O., Opperdoes, F.R. Preliminary crystallographic studies of triosephosphate isomerase from the blood parasite *Trypanosoma brucei brucei*. J. Mol. Biol. 178:487–490, 1984.
12. Tronrud, D.E., Ten Eyck, L.F., Matthews, B.W. An efficient general-purpose least-squares refinement program for macromolecular structures. Acta Crystallogr. A43: 489–501, 1987.
13. Read, R.J. Improved Fourier coefficients for maps using phases from partial structures with errors. Acta Crystallogr. A42:140–149, 1986.
14. Jones, T.A. Interactive computer graphics: FRODO. Methods Enzymol. 115:157–171, 1985.
15. Wierenga, R.K., Swinkels, B.W., Michels, P.A.M., Osinga, K., Misset, O., van Beeumen, J., Gibson, W.C., Postma, J.P.M., Borst, P. Opperdoes, F.R., Hol, W.G.J. Common elements on the surface of glycolytic enzymes from *Trypanozoma brucei* may serve as topogenic signals for import into glycosomes. EMBO J. 6:215–221, 1987.
16. Schreuder, H.A., Van der Laan, J.M., Wierenga, R.K. The transfer of protein crystals from their original mother liquor to a solution with a completely different precipitant. J. Appl. Crystallogr. 21:426–429, 1988.
17. Pflugrath, J.W., Messerschmidt, A. MADNES: Users Guide. Max-Planck-Institut für Biochemie, Martinsried, Federal Republic of Germany, 1986.
18. Brünger, A.T., Kuriyan, J., Karplus, M. Crystallographic R factor refinement by molecular dynamics. Science 235: 458–460, 1987.
19. Fujinaga, M., Gros, P. and van Gunsteren, W.F. Testing the method of crystallographic refinement using molecular dynamics. J. Appl. Crystallogr. 22:1—8, 1989.
20. Gros, P., Fujinaga, M., Dijkstra, B.W., Kalk, K.H., Hol, W.G.J. Crystallographic refinement by incorporation of molecular dynamics: Thermostable serine protease thermithase complexed with Eglin C. Acta Crystallogr. B45:488–499, 1989.
21. Berendsen, H.J.C., Postma, J.P.M., van Gunsteren, W.F., Dinola, A., Haak, J.R. Molecular dynamics with coupling to an external bath. J. Chem. Phys. 81:3684–3690, 1984.
22. Van Gunsteren, W.F., Berendsden, H.J.C. Algorithms for macromolecular dynamics and constraint dynamics. Mol. Phys. 34:1311–1327, 1977.
23. Brünger, A.T., Karplus, M., Petsko, G.A. Crystallographic refinement by simulated annealing: Application to crambin. Acta Crystallogr. A45:50–61, 1989.
24. Fermi, G., Perutz, M.F., Shaanen, B., Fourme, R. The crystal structure of human deoxyhaemoglobin at 1.74Å resolution. J. Mol. Biol. 175:159–174, 1984.
25. Bernstein, F.C., Koetzle, T.F., Williams, G.J.B., Meyer, E.F., Brice, M.D., Rodgers, J.R., Kennard, O., Shimanouchi, T., Tasumi, M. The Protein Data Bank: A computer-based archival file for macromolecular structures. J. Mol. Biol. 112:535–542, 1977.
26. Suguna, K., Bott, R.R., Padlan, E.A., Subramanian, E., Sheriff, S., Cohen, G.H., Davies, D.R. Structure and refinement at 1.8Å resolution of the aspartic proteinase from Rhizopus Chinensis. J. Mol. Biol. 196:877–900, 1987.
27. Creighton, T. "Proteins." New York: Freeman and Company, 1983.
28. Alber, T.C., Davenport, R.C., Jr., Giammona, D.A., Lolis, E., Petsko, G.A., Ringe, D. Crystallography and site-directed mutagenesis of yeast triosephosphate isomerase: "What can we learn about catalysis from a 'simple' enzyme?" Cold Spring Harbor Symp. Quant. Biol. 52:603–613, 1987.
29. Kabsch, W., Sander, C. Dictionary of protein structure: Pattern recognition of hydrogen-bonded and geometrical features. Biopolymers 22:2577–2637, 1983.
30. Lolis, E., Alber, T., Davenport, R.C., Rose D., Hartmann, F.C., Petsko, G.A. Structure of yeast triosephosphate isomerase at 1.9Å resolution. Biochemistry 29:6609–6618, 1990.
31. Lolis, E., Petsko, G.A. Crystallographic analysis of the complex between triosephosphate isomerase and 2-phosphoglycolate at 2.5Å resolution: implications for catalysis. Biochemistry 29:6619–6625, 1990.
32. Noble, M.E.M., Wierenga, R.K., Lambeir, A-M., Opperdoes, F.R., Thunnissen, A.M.W.H., Kalk, K.H., Groendijk, H., Hol, W.G.J. The adaptability of the active site of trypanosomal triosephosphare isomerase as observed in the cystal structures of three different complexes. Proteins 10: 50–69, 1991.
33. Pompliano, D.L., Peyman, A., Knowles, J.R. Stabilization of a reaction intermediate as a catalytic device: definition of the functional role of the flexible loop in triosephosphate isomerase. Biochemistry 29:3186–3194, 1990.